

Chitosan-elicited defense responses in Cucumber mosaic virus
(CMV)-infected tomato plants

Peer-reviewed author version

Rendina, Nunzia; Nuzzaci, Maria; Scopa, Antonio; CUYPERS, Ann & Sofo, Adriano
(2019) Chitosan-elicited defense responses in Cucumber mosaic virus
(CMV)-infected tomato plants. In: Journal of Plant Physiology, 234, p. 9-17.

DOI: 10.1016/j.jplph.2019.01.003

Handle: <http://hdl.handle.net/1942/29729>

Chitosan-elicited defense responses in *Cucumber mosaic virus* (CMV)-infected tomato plants

Nunzia Rendina^{a*}, Maria Nuzzaci^a, Antonio Scopa^a, Ann Cuypers^b, Adriano Sofo^a

^a School of Agricultural, Forestry, Food and Environmental Sciences, University of Basilicata, Viale dell' Ateneo Lucano, 10, 85100 Potenza, Italy

^b Environmental Biology, Centre for Environmental Sciences, Hasselt University, Agoralaan, Building D, 3590 Diepenbeek, Belgium

* Corresponding author: nunzia.rendina@unibas.it (Nunzia Rendina) School of Agricultural, Forestry, Food and Environmental Sciences, University of Basilicata, Viale dell' Ateneo Lucano, 10, 85100 Potenza, Italy

nunzia.rendina@unibas.it (Nunzia Rendina); maria.nuzzaci@unibas.it (Maria Nuzzaci); antonio.scopa@unibas.it (Antonio Scopa); ann.cuypers@uhasselt.be (Ann Cuypers); adriano.sofo@unibas.it (Adriano Sofo)

Abbreviations: *A*, photosynthetic activity; ANOVA, analysis of variance; AR156, *Bacillus cereus* AR156; CERK1, chitin elicitor receptor kinase 1; CHT, chitosan; CMV, *Cucumber mosaic virus*; DAS-ELISA, double-antibody sandwich enzyme-linked immunosorbent assay; ET, ethylene; F_v/F_m , maximum quantum yield of PSII; GAPDH, glyceraldehyde-3-phosphate dehydrogenase; g_s , stomatal conductance to water vapor; ISR, induced systemic resistance; JA, jasmonic acid; NPR1, non-expressor of pathogenesis-related genes 1; ϕ PSII, quantum yield of PSII; PAL, phenylalanine ammonia lyase; PAR, photosynthetically active radiation; PR, pathogenesis-related; PSY, phytoene synthase; PVX, *Potato virus X*; qPCR, Real-Time quantitative PCR; ROS, reactive oxygen species; SA, salicylic acid; SAR, systemic acquired resistance; TMV, *Tobacco mosaic virus*; TP, treated plants; TUB, tubulin; UK, uridylate kinase

ABSTRACT

The control of plant diseases by inducing plant resistance responses represents an interesting solution to avoid yield losses and protect the natural environment. Hence, the intertwined relationships between host, pathogen and inducer are increasingly subject of investigations. Here,

we report the efficacy of chitosan-elicited defense responses in *Solanum lycopersicum* var. *cerasiforme* plants against *Cucumber mosaic virus* (CMV). Chitosan was applied via foliar spray before the CMV inoculation to verify its effectiveness as a preventive treatment against the viral infection. Virus accumulation, photosynthetic performance, as well as genes encoding for proteins affecting resistance responses and biosynthetic pathways, were investigated. It was observed a significant reduction of CMV accumulation in chitosan-treated plants that were successively infected with CMV, compared to only CMV-infected ones (up to 100%). Similarly, a positive effect of chitosan on gas exchange dynamics was revealed. The analysis of gene expression (*CEVI-1*, *NPRI*, *PSY2* and *PAL5*) suggested the occurrence of chitosan-induced, systemic acquired resistance-related responses associated with a readjustment of the plant's oxidative status. In addition, the absence of deleterious symptoms in chitosan-treated successively CMV-infected plants, confirmed that chitosan can be used as a powerful control agent. Our data indicate that chitosan, when preventively applied, is able to elicit defense responses in tomato to control CMV infection. Such finding may be recommended to protect the tomato fruit yields as well as other crops.

Keywords: Chitosan; *Cucumber mosaic virus*; Defense/antioxidant-related protein; Disease control; Photosynthetic performance; *Solanum lycopersicum* var. *cerasiforme*.

1 Introduction

Plants are susceptible to numerous pathogens responsible for diseases that can reduce crop yield (e.g., (Vitti et al., 2015)), causing severe economic losses. Among the most dangerous phytopathogens, viruses cannot be faced by using specific agrochemicals (Iriti and Varoni, 2015).

Hence, control of viral infections, protecting the natural environment, is the best strategy to ensure an, at least, satisfactory harvest. In such a scenario, elicitors triggering plant defense responses and inducing a systemic resistance state can represent a solution.

Chitosan (CHT) is a polycationic heteropolysaccharide composed by N-acetyl-D-glucosamine and D-glucosamine linked by β -(1 \rightarrow 4) glycosidic bonds (Iriti and Varoni, 2015). Although CHT is a natural compound (present in Zygomycetes), it is mainly obtained by the deacetylation of chitin, a component of the fungal cell wall and the arthropod exoskeleton (Iriti and Varoni, 2015). Chitosan polymers may vary in molecular weight, viscosity, pKa value, polymerization and deacetylation degree, affecting their physicochemical and biological properties (Iriti and Varoni, 2015). Chitosan is a biodegradable and nontoxic compound inducing systemic acquired resistance (SAR) to pathogens in plants (Xing et al., 2015). This compound also exhibits a direct antimicrobial activity, likely mainly through electrostatic interactions (Xing et al., 2015). Chitosan bioactivities can be explained because the polycationic nature of CHT leads to affinity with the anionic contents of target organism (Kumaraswamy et al., 2018). More specifically, as an antimicrobial, CHT interaction with cell wall and cell membranes can destabilize them. In addition, its interaction with DNA and proteins can interfere with the transcription and translation mechanisms (Kumaraswamy et al., 2018). Furthermore, CHT can chelate essential nutrients, trace elements and metal ions that are necessary for the microbial growth, as well as it can form a polymer film that compromises metabolite excretion and nutrient uptake (Xing et al., 2015). However, the detailed mechanism of action of CHT in reducing plant diseases has not been completely revealed (Hassan and Chang, 2017). Chitosan perception by plant is shortly followed by a variation in the ion fluxes and membrane depolarization (Iriti and Varoni, 2015). Therefore, CHT can be recognized by plant as a pathogen-mimicking stimulus, but the identification of a CHT receptor is still doubtful (Malerba and Cerana, 2016; Povero et al., 2011). Although Petutschnig et al. (2010) found that the chitin elicitor receptor kinase 1 (CERK1) also bound more weakly to CHT, later Povero et al. (2011)

demonstrated that the perception of CHT was independent of CERK1. Recently, Liu et al. (2018) suggested wheat W5G2U8, W5HY42, and W5I0R4 as potential chitosan oligosaccharides receptors. Interestingly, the application of CHT to promote the plant growth has also been studied (Kumaraswamy et al., 2018; Sharif et al., 2018) and CHT nanoparticles can also be used to deliver pesticides, herbicides, fertilizers, micronutrients as well as genetic material (Malerba and Cerana, 2016). The antimicrobial activity of CHT has been studied for bacteria, yeasts and moulds (Liu et al., 2004). Furthermore, CHT is effective as an alternative treatment to conventional fungicides aimed to control the postharvest decay, both after preharvest (Feliziani et al., 2015) and postharvest applications. The latter is associated with CHT coating of fruits (Sivakumar et al., 2016). On cherry tomato fruit, CHT exerted an inhibitive action on the gray mold (*Botrytis cinerea*), presumably involving the mitogen-activated protein kinase signaling pathway and determining an increase of hydrogen peroxide, peroxidase activity, as well as *PR1a1* and *PR5* transcripts (Zhang et al., 2015). Chitosan-induced responses against viruses, such as *Potato virus X* (PVX) and *Tobacco mosaic virus* (TMV), were also evaluated (Chirkov et al., 2001; Jia et al., 2016; Nagorskaya et al., 2014). *Cucumber mosaic virus* (CMV) (genus *Cucumovirus*, family *Bromoviridae*) presents polyhedral virions composed of 180 subunits (T=3 icosahedral symmetry) (Gallitelli, 1998). Virus particles are isometric: separate particles separately contain RNA1 and RNA2, a third particle contains RNA3 and subgenomic RNA4 (Agrios, 1997) and possibly RNA3 and subgenomic RNA4A (Gallitelli, 2000). RNA1 and RNA2 code for two different proteins involved in RNA replication (Agrios, 1997). The 2b protein is translated from the RNA4A of RNA2 (Gallitelli, 2000). RNA3 encodes a protein involved in virus movement and contains the open reading frame for the coat protein. The coat protein cistron is translated via the RNA4 (Gallitelli, 2000). In order to infect plants, the co-infection with the three particles together is required (Gallitelli, 1998). The numerous strains belonging to CMV differ in properties and characteristics such as host plants, symptoms produced, ways of transmission (Agrios, 1997). Infecting at least 100 plant families and 1,200 species

(Edwardson and Christie, 1991), CMV has a wide range of hosts, such as ornamentals and many species of vegetables (Agrios, 1997). Furthermore, CMV causes distortion and discoloration of leaves, fruits and flowers, reduction in quantity and quality of crop yield, up to reduced growth and plant death (Agrios, 1997). It is known that about 80 species of aphids can represent vectors of CMV. For this reason, control approaches can include the removal of aphids and the destruction of CMV reservoirs weeds (Gallitelli, 1998). Interestingly, CMV, *Alfalfa mosaic alfamovirus* (AMV), *Potato M carlavirus* (PVM), *Potato Y potyvirus* (PVY) and *Tomato spotted wilt tospovirus* (TSWV) often compose mixed infections in tomato cultivated in the Mediterranean basin (Gallitelli, 1998). Limited information has been reported on the tools and mechanisms controlling the virus diseases, especially regarding the economically relevant CMV. Specifically, a gap exists in the complete understanding of the tomato-CMV-CHT interaction. For this reason, the viral titer, the plant photosynthetic performance and the expression of genes related to antioxidant compounds and plant resistance responses to pathogens, were investigated in tomato plants infected with CMV, with and without CHT treatment. Therefore, the aim of this work was to investigate the efficacy of CHT as an innovative and eco-friendly strategy to elicit defense responses in tomato plants against CMV, so avoiding the negative consequences of the viral infection.

124

125 **2 Materials and methods**

126 **2.1 Chitosan (CHT) and CMV sources and preparations**

127

128 Low molecular weight CHT (50-190 kDa, 75-85% deacetylated) was purchased from Sigma-
129 Aldrich (448869; St. Louis, MO, USA). Chitosan (1 g) was dissolved in distilled water (40 mL)
130 containing 1 M acetic acid (9 mL) under overnight continuous stirring. The pH was 5.4. Eliciting
131 CHT solution was prepared by dissolving 1 g of this stock in 1 L of distilled water and foliar

sprayed (10 mL plant⁻¹), while water was sprayed on untreated plants. Obtained as reported by Vitti et al. (2015), *Cucumber mosaic virus* strain Fny inducing necrosis (CMV-Fny) was propagated in *Nicotiana tabacum* cv Xanthi plants. Subsequently, tobacco leaves exhibiting CMV-Fny symptoms were macerated in 0.05 M sodium citrate buffer (pH 6.5) and the suspension was mechanically rubbed on celite pre-dusted tomato leaves.

2.2 Experimental setup

Solanum lycopersicum var. *cerasiforme* seeds were sterilized (1 min in 1% Na-hypochlorite solution) and then put to germinate on moist filter paper imbibed with sterile distilled water in Petri dishes. After incubation for 24 h at 4 °C in the dark and for 2-3 days at 26 °C, seedlings were transferred to pots filled with sterilized soil. At the four-leaf stage, plants were transplanted and grown in a greenhouse at a temperature regime of 26/23 °C (day/night) and with a 16-h photoperiod.

The experimental design included four experimental conditions (15 plants for each condition): untreated plants; plants inoculated with CMV (CMV-TP); plants treated with CHT (CHT-TP); plants treated with CHT and then inoculated with CMV 24 h after CHT treatment (CHT-CMV-TP). Treatment/inoculation was performed starting from the tenth day after transplantation.

2.3 CMV determination

Twenty and ninety days after CMV inoculation, leaves from three plants randomly chosen, were collected and used for a double-antibody sandwich enzyme-linked immunosorbent assay (DAS-ELISA) according to Vitti et al. (2016). Measurements were performed spectrophotometrically

156 (model Multiskan GO: Thermo Fisher Scientific, Waltham, MA, USA) and the mean absorbance
157 value ($OD_{405\text{ nm}}$) of six replicates for each experimental condition was taken.

158

159 **2.4 Gas exchange and chlorophyll fluorescence**

160

161 Photosynthetic activity (A), stomatal conductance to water vapor (g_s), maximum quantum yield of
162 PSII (F_v/F_m) (dark-adapted state) and quantum yield of PSII (ϕ PSII) (light-adapted state) were
163 measured on clear days. Two apical fully developed leaves, belonging to one of three (for A and g_s
164 determinations) or of two (for F_v/F_m and ϕ PSII determinations) 2- and 4-month-old plants randomly
165 chosen for each experimental condition, were tested. Measurements were carried out using the LI-
166 6400 portable photosynthesis system (LI-COR, Lincoln, NE, USA), operating between 10:00 and
167 12:00 a.m., at 398 ppm external CO_2 concentration, flow rate at $500\text{ }\mu\text{mol s}^{-1}$ and $1500\text{ }\mu\text{mol}$
168 $\text{photons m}^{-2}\text{ s}^{-1}$ photosynthetically active radiation (PAR). Temperature inside the leaf chamber was
169 maintained equal to environmental air temperature ($28\text{ }^{\circ}\text{C}$) by instrument automatic temperature
170 regulation.

171 The same plants used for gas exchange measurements were chosen to measure chlorophyll
172 fluorescence at 10:00-12:00 a.m. using a leaf chamber fluorometer (LI-6400-40; Li-Cor, Inc.). On
173 each plant, both sun-adapted and dark-adapted leaves were chosen to measure fluorescence
174 parameters. On dark-adapted leaves (covered by silver film for 18 h before the measurements by
175 homemade clip holders), the maximum quantum yield of PSII photochemistry was calculated as
176 $F_v/F_m = (F_m - F_o)/F_m$ (Murchie and Lawson, 2013), where F_m is the maximum fluorescence in the
177 dark and F_o is the minimum level of fluorescence. On sun-adapted leaves, the quantum yield of PSII
178 (ϕ PSII) was calculated as $(F_m' - F')/F_m'$ (Murchie and Lawson, 2013), where F_m' is the maximum
179 fluorescence in the light and F' is the steady-state fluorescence yield measured under actinic light.
180 The value of PAR inside the leaf chamber (light with a 90% red fraction at a wavelength of 630 nm

181 and a 10% blue fraction at 470 nm) during fluorescence measurements was $950 \mu\text{mol m}^{-2} \text{s}^{-1}$. This
182 value was chosen keeping into account (1) the measured average light saturation point (900 to 1000
183 $\mu\text{mol m}^{-2} \text{s}^{-1}$) and (2) the mean environmental irradiance monitored by the LI-6400 external
184 quantum light sensor every 3 seconds.

185

186 **2.5 SPAD measurements**

187

188 Leaf chlorophyll content was measured with a portable meter (SPAD-502, Minolta Camera Co.
189 Ltd., Osaka, Japan) between 10:00 and 11:00 a.m. Three apical fully developed leaves, belonging to
190 one of two 2- and 4-month-old plants randomly chosen for each condition were tested. The mean
191 value of the six measurements was recorded.

192

193 **2.6 Extraction and determination of total phenolic content**

194

195 Extractions and determinations were carried out in two randomly chosen plants for each condition,
196 analyzing leaves collected 60 h after the only or last treatment/inoculation. The total phenolic
197 content was analyzed spectrophotometrically using the Folin-Ciocalteu reagent and catechol as
198 standard, as reported by Sofo et al. (2017). All values were expressed as mg catechol equivalents
199 100 g^{-1} of leaves fresh weight. The mean absorbance value ($\text{OD}_{650 \text{ nm}}$) of four replicates for each
200 condition was taken.

201

202 **2.7 Gene expression analysis**

203

204 Frozen leaves collected nine days after the only or last treatment/inoculation, from one of four 1.5-
205 month-old plants for each experimental condition, were ground in liquid nitrogen in a

206 pestle and mortar. From the powder obtained, RNA was extracted using the RNAqueous Total RNA
207 Isolation kit (AM1912, Ambion, Life Technologies, Thermo Fisher Scientific, Waltham, MA,
208 USA). On ice, RNA was purified adding 1/10 volume of 3M sodium acetate and 7/10 volume of
209 100% isopropanol. Samples were stored at -80°C for 30 min, then centrifuged at 4°C for 15 min
210 at maximum speed. To the pellet saved, 400 μL of 70% ethanol was added and two centrifugations
211 at 4°C for 2 min at maximum speed taking off the supernatant were carried out. The open tubes
212 were put at 37°C for 5 min in a heat block (ThermoStat Plus, Eppendorf, Hamburg, Germany) and
213 finally, RNase-free water was added to dissolve the RNA pellet. Purified RNA concentration and
214 purity were spectrophotometrically determined at 260 nm (NanoDrop ND-1000 UV/Vis
215 Spectrophotometer, NanoDrop Technologies, Wilmington, DE, USA). The Experion RNA StdSens
216 Analysis Kit (Bio-Rad Laboratories, Hercules, CA, USA) was used to assess the RNA quality. To
217 the same concentration (1 μg) of all the RNA samples then utilized for the reverse transcription,
218 DNase (TURBO DNA-free Kit, AM1907, Invitrogen, Thermo Fisher Scientific, Waltham, MA,
219 USA) was added to degrade contaminating gDNA. cDNA synthesis was carried out starting from
220 oligo(dT)-primers and random hexamers (PrimeScript RT Reagent Kit, Perfect Real Time,
221 RR037A, Takara, Japan), then the cDNA obtained was 10-fold diluted using 1/10 TE buffer (1 mM
222 Tris-HCl, 0.1 mM EDTA, pH 8.0). Real-Time quantitative PCR (qPCR) was performed
223 coupled with SYBR Green fluorescent dye, using the 7500 Real-Time PCR System (Applied
224 Biosystems, Lennik, Belgium). Cycling conditions were 95°C for 20 s, 50 cycles of 3 s at 95°C
225 and 30 s at 60°C . A final volume of 10 μL contained 2 μL of cDNA produced, 5 μL of Fast SYBR
226 Green Master Mix (4385612, Applied Biosystems, Lennik, Belgium), 0.3 μL of each forward and
227 reverse primer (300 nM) (Table 1) and 2.4 μL of RNase-free water. A dissociation curve followed
228 to evaluate the amplification specificity. Sequences for the reference genes, as well as for the genes
229 of interest, were searched in the NCBI (<https://www.ncbi.nlm.nih.gov>) and JGI Phytozome
230 (<https://phytozome.jgi.doe.gov/pz/portal.html>) databases, and related primers were designed using

231 Primer3 Program and nBLAST-NCBI (Table 1). Primers efficiency ($E = 10^{(-1/\text{slope})} - 1$) was
232 measured using serial dilutions from 1/2 to 1/64 of cDNAs collected in a pooled sample and
233 realizing C_q versus $\log(\text{dilution})$ calibration lines (Table 2). The GrayNorm algorithm
234 (<https://github.com/gjbex/GrayNorm>) was adopted to select the combination of reference genes able
235 to yield the highest possible accuracy. The expression of the genes encoding (EC 1.11.1.7)
236 peroxidase (*CEVI-1*), non-expressor of pathogenesis-related genes 1 (*NPRI*), (EC 2.5.1.32)
237 phytoene synthase 2 (*PSY2*) and (EC 4.3.1.5) phenylalanine ammonia lyase (*PAL5*) was considered
238 relative to five reference genes selected for normalization: *SAND*, *TIP4*, *TUB* (tubulin), *UK*
239 (uridylate kinase) and *GAPDH* (glyceraldehyde-3-phosphate dehydrogenase). In Tables 1 and 2 are
240 respectively reported sequences and efficiencies of primers for the reference genes and genes of
241 interest for qPCR analysis. Genes of interest relative expression was calculated as $2^{-\Delta C_q}$, and the $2^{-\Delta C_q}$
242 values geometric average was used for data normalization.

243

244

245

246

247

248

249

250

251

252

253

254 Table 1 - Primers sequence

| Name | Sequence | Tm (°C) |
|---|---------------------------------|---------|
| <i>SAND</i> | 5'-CCAGCTAACTTTCTCCATGCTTAC-3' | 58.1 |
| | 5'-ACCAACAAGACTGATAACCTTTTGT-3' | 55.3 |
| <i>TIP4</i> | 5'-CTGTTAAAGTGAGAGTCATGCCTAG-3' | 58.4 |
| | 5'-TGCAAACGAGTGTCTCTTAGTCT-3' | 57.8 |
| <i>TUB</i> | 5'-AGAATGCCGATGAATGTATGGT-3' | 55.0 |
| | 5'-CAGGGAATCTCAAACAGCAAG-3' | 55.2 |
| <i>UK</i> | 5'-TGGTAAGGGCACCCAATGTGCTAA-3' | 59.7 |
| | 5'-ATCATCGTCCCATTCTCGGAACCA-3' | 59.9 |
| <i>GAPDH</i> | 5'-GATGTCTCCGTTGTCGATCTT-3' | 55.1 |
| | 5'-CAAGATACCCTTCAATTTACCCTCT-3' | 55.9 |
| <i>CEVI-1</i> (GenBank accession number Y19023) | 5'-TCACCAACAAGGGAATGGAT-3' | 52.0 |
| | 5'-TGGATCAGGGCTACCACTTC-3' | 54.9 |
| <i>NPR1</i> (Phytozome Solyc07g040690.2) | 5'-CGATGATTTGCGTATGAAGC-3' | 54.3 |
| | 5'-CCAGGGGTAAATTCAGACGTG-3' | 54.4 |
| <i>PSY2</i> (Phytozome Solyc02g081330.2) | 5'-CCGAATCCGAGGTCTCATA-3' | 54.5 |
| | 5'-CCTGTCTCCCACCTTTCTTG-3' | 54.5 |
| <i>PAL5</i> (GenBank accession number M90692) | 5'-CTCTGGCAATGGGTGCTAAT-3' | 55.2 |
| | 5'-CAGGGGTCATCAGCATAGGT-3' | 55.3 |

255

256

257

258

259

260

261 Table 2 - Primers efficiency

| Primer | PCR efficiency (80-120%) | Equation | R ² Coefficient |
|---------------|-----------------------------|-------------------------|-------------------------------|
| <i>SAND</i> | 93.03% | $y = -3.5010x + 25.795$ | $R^2 = 0.9923$ |
| <i>TIP4</i> | 100.51% | $y = -3.3097x + 24.447$ | $R^2 = 0.9964$ |
| <i>TUB</i> | 100.78% | $y = -3.3035x + 23.606$ | $R^2 = 0.9984$ |
| <i>UK</i> | 87.58% | $y = -3.6605x + 25.201$ | $R^2 = 0.9987$ |
| <i>GAPDH</i> | 96.92% | $y = -3.3981x + 21.682$ | $R^2 = 0.9992$ |
| <i>CEVI-1</i> | 105.70% | $y = -3.1926x + 25.276$ | $R^2 = 0.9944$ |
| <i>NPRI</i> | 103.53% | $y = -3.2401x + 25.306$ | $R^2 = 0.9997$ |
| <i>PSY2</i> | 92.89% | $y = -3.5049x + 24.470$ | $R^2 = 0.9939$ |
| <i>PAL5</i> | 100.73% | $y = -3.3045x + 22.149$ | $R^2 = 0.9990$ |

262

263

264 **2.8 Statistical data analysis**

265

266 Normal distribution of data was tested performing the Shapiro-Wilk test ($P \leq 0.05$) and
267 homoscedasticity was tested performing the Bartlett's test ($P \leq 0.05$). Data were analyzed by one-
268 and two-way analysis of variance (ANOVA). Parametric and non-parametric as multiple
269 comparisons were performed using the Tukey's HSD test and the Kruskal-Wallis test, respectively.
270 Statistical analyses were performed using the software RStudio: Integrated Development for R,
271 version 1.0.136 (RStudio, Inc., Boston, MA, USA).

272

273 **3 Results**

274

275 Twenty days after CMV inoculation, only CMV-TP showed mosaic and chlorosis in leaves, as well
276 as their deformation (Figure 1A). On the contrary, the absence of symptoms induced by CMV was

277 detected in CHT-CMV-TP (Figure 1A). Furthermore, the same four experimental conditions, with
278 the same inoculations and treatments methods, were also applied to *Nicotiana tabacum*. Eleven
279 days after CMV inoculation, tobacco CMV-TP showed mosaic in leaves, but the absence of CMV
280 symptoms was detected in tobacco CHT-CMV-TP (Figure 1B).

281

282 **3.1 CMV load**

283

284 CHT-CMV-TP showed the mean optical density value significantly lower than that determined in
285 CMV-TP, both in 20 days and 90 days after CMV inoculation determinations (–86% and –100%,
286 respectively). The absence of CMV was detected in untreated and CHT-TP, and no significant
287 difference was revealed between these two conditions (Figure 2).

288

289 **3.2 Gas exchange and chlorophyll fluorescence**

290

291 Considering the *A* value between 2- and 4-month-old plants, CMV-TP and CHT-TP showed the
292 lowest and the highest *A* value, respectively (Figure 3A). Although not significantly, CHT-CMV-
293 TP had the *A* value of 44% higher than that determined in CMV-TP, and untreated plants showed
294 the *A* value lower (–25%) than that determined in CHT-TP (Figure 3A). The 2-month-old CHT-TP
295 and CMV-TP showed the highest and the lowest *g_s* value, respectively (Figure 3B). Chitosan
296 treatment in CHT-CMV-TP caused a *g_s* value of 146% significantly higher than that determined in
297 CMV-TP, and a *g_s* value not significantly different than that determined in CHT-TP. Untreated
298 plants showed a *g_s* value not significantly different than that of CMV-TP, and a *g_s* value
299 significantly lower (–59%) than that of CHT-TP (Figure 3B). Results were not significantly
300 different between the four conditions, in 4-month-old plants (Figure 3B). The 4-month-old CHT-TP
301 and CHT-CMV-TP showed a significant decrease in the *g_s* value, compared to the *g_s* value of 2-

month-old plants (–58 and –50%, respectively) (Figure 3B). The 4-month-old CMV-TP showed the lowest F_v/F_m value, lower (–6%) than the average value of the F_v/F_m values of all the other conditions (Figure 3C). The 4-month-old CMV-TP also showed a significant decrease of the F_v/F_m value, compared to that determined in 2-month-old plants (–7%) (Figure 3C). The 4-month-old untreated, CHT-TP and CHT-CMV-TP showed a significant increase in the ϕ PSII value, compared to that of 2-month-old plants (298, 217 and 218%, respectively) (Figure 3D).

3.3 SPAD

In 2-month-old plants, CHT-TP had a SPAD value 11% significantly higher than that found in untreated plants. Finally, among 4-month-old plants, the CHT-CMV-TP showed the lowest SPAD value (Figure 4).

3.4 Total phenolic content

Untreated plants and CHT-CMV-TP showed the highest and the lowest total phenolic content, respectively. CHT-CMV-TP showed a total phenolic content significantly lower than that determined in untreated and CMV-TP (–41 and –40%, respectively) (Figure 5).

3.5 Gene expression analysis

Reference genes were TUB, UK and GAPDH for the experimental conditions represented in Figure 6; SAND, TIP4 and GAPDH for those represented in Figure 7.

Untreated plants were assumed as a control, compared to CMV-TP, and no significant difference was found in the relative expression of all the genes of interest assayed (Figure 6). Although not

327 significant, an increase in *CEVI-1* transcripts was detected in the leaves of CMV-TP (Figure 6A).
328 Finally, *PAL5* expression was the most stable in the considered conditions (Figure 6).
329 CMV-TP were then assumed as a control, compared to CHT-TP and CHT-CMV-TP (Figure 7). A
330 significant increase in *PAL5* expression was observed both in CHT-TP and CHT-CMV-TP,
331 compared to CMV-TP (Figure 7D). Conversely, no significant up-regulation of *NPRI* and down-
332 regulation of *CEVI-1* and *PSY2* transcripts were observed (Figures 7B, A and C, respectively).

333

334 **4 Discussion**

335

336 The plant-virus interaction affects the chloroplast. More specifically, the virus replication and viral
337 movement involve chloroplast factors (Zhao et al., 2016). As a result, the chloroplast structure and
338 the expression of photosynthesis-related proteins are perturbed as well as the viral symptoms are
339 manifested (Zhao et al., 2016).

340 Studies have shown the efficacy against strains of CMV infection of treatment with *Trichoderma*
341 *harzianum* T-22 (Vitti et al., 2016, 2015), *Paenibacillus lentimorbus* B-30488 (Kumar et al., 2016)
342 and benzo-(1,2,3)-thiadiazole-7-carbothioic acid *S*-methyl ester (BTH) (Anfoka, 2000).

343 The present research investigated the ability of CHT to elicit defense response in tomato plants
344 inoculated with CMV.

345

346 **4.1 CMV symptoms and load monitoring**

347

348 A phenotypical observation showed the capacity of CHT to control CMV symptoms, testing tomato
349 and tobacco as host plants. Indeed, neither tomato nor tobacco CHT-treated then CMV-infected
350 plants displayed viral infection symptoms (Figures 1A and B, respectively). The results of DAS-

351 ELISA showed the efficacy of CHT to control foliar CMV load in tomato CHT-CMV-TP, both at
352 20 days and at 90 days after CMV inoculation measurements (Figure 2). In agreement with our
353 results, determined by ELISA, a CHT-induced resistance in potato against PVX was suggested as
354 probably mediated by the enhanced ribonuclease activity and callose deposition (Chirkov et al.,
355 2001). Furthermore, in *Nicotiana tabacum* L. cv. Samsun leaves, Nagorskaya et al. (2014) showed
356 that CHT limited TMV coat protein content and infectivity as well as increased the hydrolases
357 (proteases and RNases) activity. They also detected a highest content of abnormal virions.

358

359 **4.2 Plant physiological responses to CHT and CMV**

360

361 Photosynthetic activity was considerably analogous, between the short and long term (when plants
362 were 2- and 4-month-old, respectively). Although not significantly, CHT treatment improved the
363 photosynthetic activity (Figure 3A). Van et al. (2013) reported the effects of CHT nanoparticles on
364 Robusta coffee and, according to our results, they found an enhanced photosynthesis net rate and
365 besides, they supposed increased stomatal cells opening degree and stomatal conductance because
366 of the polycation property of CHT that raise the osmosis pressure of stomatal cells. Salachna et al.
367 (2017) suggested that the positive effect of CHT on plant growth parameters may cause the
368 increased stomatal conductance with CHT foliar application. However, the reduction of stomatal
369 apertures width after foliar CHT treatment of bean has also been reported (Iriti et al., 2009).
370 Differently from *A* data, effect of treatment/inoculation on stomatal conductance was more evident
371 when plants were 2-month-old (Figure 3B). As reported by Vitti et al. (2016), the 2-month-old
372 tomato plants inoculated with CMV showed reduced stomatal conductance to water vapor besides
373 decreased photosynthetic activity (Figures 3B and A, respectively).

374 In agreement with the results obtained by Marler et al. (1993) on papaya leaves inoculated with
 375 *Papaya ringspot virus* (PRV), a significantly lower maximal quantum yield of PSII value (F_v/F_m)
 376 was detected in CMV-TP than untreated ones, in 4-month-old plants (Figure 3C), probably
 377 indicating a damage to PSII or photoinactivation caused by a decrease of the opened reaction
 378 centers. The quantum yield of PSII values detected in 4-month-old plants were higher (some
 379 significantly) than ones detected in 2-month-old plants (Figure 3D). No significant influence of
 380 CHT treatment was recorded in F_v/F_m ratio and similarly occurred in ϕ PSII value, compared to
 381 untreated and only infected plants (CMV-TP) (Figures 3C and D, respectively).
 382 SPAD meter measures the relative chlorophyll content by estimating the leaf greenness. Indeed,
 383 chlorophyll reflects a green light, inducing this color in plants (Shi et al., 2018). Results indicated
 384 no significant difference in SPAD readings of CMV-TP, compared to untreated plants, in the same
 385 interval measurements. However, in 4-month-old plants, CMV-TP had a SPAD value lower than
 386 that of untreated plants, reflecting the changed pigmentation responsible for the symptoms
 387 displayed. Furthermore, our data indicated that CHT-TP showed a significant increase in
 388 chlorophyll content, compared to untreated ones, in 2-month-old plants (Figure 4). Van et al. (2013)
 389 also reported that CHT nanoparticles improved the content of chlorophylls as well as the uptake of
 390 nitrogen and magnesium that constitute the chlorophyll chemical structure.
 391 Phenols produced by plants vary in the defense response against environmental stresses (Sofo et al.,
 392 2017). In our case, 60 h after CMV inoculation, foliar total phenolic content was not significantly
 393 different between CMV-TP and untreated plants (Figure 5). The same result was obtained six days
 394 after the inoculation of CMV-Y in tobacco plants (Ipper et al., 2008). Furthermore, the treatment
 395 with CHT, both alone and before CMV inoculation (CHT-TP and CHT-CMV-TP, respectively),
 396 caused a decrease of total phenols, compared to ones determined in only infected and untreated
 397 plants (Figure 5). In agreement with our result, Coqueiro et al. (2011) assessed the effect of low
 398 molecular weight CHT in tomato plants, then inoculated with *Xanthomonas gardneri* three days

399 after CHT treatment. They observed that the total phenolic compounds of the CHT-treated plants
400 increased starting from the second day after the inoculation of *Xanthomonas gardneri*, hence neither
401 before nor within 24 h after inoculation. Therefore, in our case, the absence of a CHT-conditioned
402 accumulation of phenolics as a response to CMV in CHT-CMV-TP may be due to the chosen
403 timing between CHT application and CMV inoculation (24 h) and/or between inoculation and
404 analysis (60 h).

405

406 **4.3 Expression analysis of defense-related genes**

407

408 The systemic acquired resistance (SAR) provides to the plant a long-lasting systemic resistance to
409 consecutive infections by many pathogens (Mou et al., 2003). The SAR involves plant responses,
410 such as the production of reactive oxygen species (ROS) and pathogenesis-related (PR) proteins, as
411 well as the lignification and cell wall reinforcement through the cell wall structural proteins cross-
412 linking (Pandey et al., 2017). More specifically, the CHT-induced resistance can enhance the
413 activities of defense-related enzymes, such as peroxidase, PAL, polyphenol oxidase, superoxide
414 dismutase and catalase (Xing et al., 2015). The induced systemic resistance (ISR) is triggered by
415 some bacteria and fungi and requires jasmonic acid (JA) and ethylene (ET). Differently, the SAR
416 requires salicylic acid (SA), exogenously applied (Mou et al., 2003) or endogenously produced.
417 To optimize the GrayNorm output for the molecular analysis, the four different experimental
418 conditions were divided into two groups (Figures 6 and 7). It was appropriate to compare the
419 expression of the assayed genes in CHT-TP and CHT-CMV-TP to untreated plants. Such
420 comparison denoted that CHT treatment causes an up-regulation of *CEVI-1*, *NPR1* and *PAL5*
421 expressions, whereas the increase of *PSY2* is only observed in even infected plants.
422 Particularly, peroxidases are enzymes that catalyze the hydrogen peroxide (H₂O₂) decomposition
423 oxidating many phenolic and non-phenolic substrates (Pandey et al., 2017). The implication of plant

424 peroxidases in processes, such as lignification, suberization, cell wall metabolism, defense against
 425 pathogens and ROS metabolism is well-known (Pandey et al., 2017). Although not statistically
 426 different, a strong increase in *CEVI-1* expression occurred in CMV-TP, compared to untreated
 427 plants (Figure 6A). Such finding is in accordance with the observation that at seven days post
 428 *Tomato mosaic virus* (ToMV) inoculation of tomato plants, *CEVI-1* expression was induced in
 429 leaves (Mayda et al., 2000). *CEVI-1* expression strong up-regulation could be associated with the
 430 cell wall reinforcement and the ROS content. Mayda et al. (2000) also reported that were able to
 431 induce *CEVI-1* expression neither incompatible interactions nor some infiltrated signal molecules.
 432 Compared to CMV-TP, the CHT treatment in CHT-CMV-TP seemed to limit the *CEVI-1*
 433 transcripts amount (Figure 7A), suggesting that CHT plays a role in the regulation of the ROS
 434 levels, thus controlling such CMV infection effect.

435 Cytosolic non-expressor of pathogenesis-related genes 1 (NPR1) regulates the salicylate- and
 436 jasmonate-dependent pathways cross-talk (Spoel et al., 2003). Moreover, in *Arabidopsis*, *Bacillus*
 437 *cereus* AR156-induced ISR to *Botrytis cinerea* required *NPR1* and JA/ET-signaling pathway (Nie et
 438 al., 2017). Interestingly, another study demonstrated that SAR induction by AR156 required *NPR1*
 439 and SA-signaling pathway (Niu et al., 2016). Wu et al. (2012) suggested that *Arabidopsis* NPR1
 440 binds SA through cysteines^{521/529} via copper. Just during SAR, NPR1 activates the PR gene
 441 expression (Mou et al., 2003). In our study, the expression of *NPR1* was analyzed as well, but no
 442 significant differences in the transcripts amount were detected (Figures 6B and 7B). However,
 443 *NPR1* expression was slightly up-regulated in CHT-TP and CHT-CMV-TP, compared to CMV-TP
 444 (Figure 7B) and untreated ones. This could indicate the CHT efficacy against CMV by triggering
 445 SAR-related defense responses in tomato plants. Jia et al. (2016) reported that CHT oligosaccharide
 446 pretreatment induced TMV resistance in *Arabidopsis* through the SA signalling pathway. An
 447 optimal low concentration (50 mg L⁻¹) applied one day before TMV inoculation was used.

448 Interestingly, Doares et al. (1995) observed an increase in the level of JA in leaves of excised
 449 tomato plants after supplying CHT oligosaccharides.

450 Photosynthesis and photoprotection are processes involving plant carotenoids (Giorio et al., 2008).
 451 The first biosynthetic step of carotenoids involves two molecules of geranylgeranyl pyrophosphate
 452 (GGPP) and is catalyzed by the enzyme phytoene synthase (PSY), that is encoded by *PSY2* in
 453 chloroplasts and *PSY1* of chromoplasts in tomato. From phytoene, sequential reactions differently
 454 form lycopene and then cyclic carotenoids such as lutein, zeaxanthin and violaxanthin (Fraser and
 455 Bramley, 2004; Giorio et al., 2008; Meléndez-Martínez et al., 2010). However, such two genes
 456 encode PSY2 and PSY1, respectively (Giorio et al., 2008). In our case, *PSY2* expression was up-
 457 regulated in CMV-TP, but such a result was not significant; On the whole, no significant difference
 458 was observed in the *PSY2* transcript amount (Figures 6C and 7C). Interestingly, Ibdah et al. (2014)
 459 found that CMV-Fny infection caused an increased phytoene content in *Nicotiana tabacum* L. cv.
 460 Samsun NN roots; however, the carotenoid production was reduced because the enzyme phytoene
 461 desaturase was down-regulated by CMV.

462 Additionally, phenylalanine ammonia lyase (PAL) converts the L-phenylalanine to ammonia and
 463 trans-cinnamic acid. PAL-catalyzed reaction is the first in phenylpropanoid metabolism. Lee et al.
 464 (1994) demonstrated that multiple initiation sites in *PAL5* allow the tomato plant to respond to
 465 different environmental stimuli in a tissue-specific fashion. In our experiment, a significant increase
 466 in *PAL5* expression occurred in CHT-TP and CHT-CMV-TP, compared to CMV-TP (Figure 7D).
 467 Such a result is in accordance with Mejía-Teniente et al. (2013), who observed that after the first
 468 CHT treatment in *Capsicum annuum* L., PAL activity as well as *pal* expression increased. No
 469 significant difference was observed in *PAL5* expression level in CMV-TP, compared to untreated
 470 plants (Figure 6D). Ogawa et al. (2006) found increased *PAL A* and *PAL B* transcripts as well as
 471 PAL activity in TMV-infected (hypersensitive reaction lesion-bearing) tobacco leaves, suggesting
 472 the phenylalanine pathway as the main route of SA synthesis. Compared to CMV-TP, the

473 significantly higher *PAL5* expression detected in CHT-CMV-TP (Figure 7D), suggests the
474 involvement of phenylpropanoid-derived products as lignin and SA.
475 The RNA silencing participates in the antiviral plant mechanism, though it is overcome by the
476 viruses encoding RNA silencing suppressors (Carr et al., 2010), such as the 2b protein of CMV.
477 Unfortunately, how virus infection is controlled in plants exhibiting SAR has not
478 been fully understood (Carr et al., 2010).

479

480 **5 Conclusions**

481

482 This paper reports the ability of chitosan as a preventive treatment able to elicit defense responses in
483 tomato plants against CMV-Fny infection. Chitosan was able to reduce the CMV titer and improved
484 the gas exchange of the infected plants. Furthermore, a SAR-related response induced by chitosan,
485 also by influencing the plant oxidative status, is hypothesizable. Such findings represent a new and
486 additional piece of the puzzle depicting effective, sustainable and environmentally safe methods of
487 plant disease control. Further studies could clearly define the whole set of the resistance responses
488 triggered specifically in such host-pathogen-elicitor combination.

489

490 **Conflict of interest statement**

491 Declarations of interest: none.

492

493 **Funding**

494 This research did not receive any specific grant from funding agencies in the public, commercial, or
495 not-for-profit sectors.

496

497 **Acknowledgments**

498 We gratefully thank Els Keunen, Stefanie De Smet, Rafaela Amaral dos Reis, Sophie Hendrix and
499 Jana Deckers for their statistical and technical support.

500

501

502

503

504

505

506

507

508

509

510

511

512

513

514

515

516

517 **References**

518

519 Agrios, G.N., 1997. Plant Pathology, fourth ed. Academic Press, San Diego.

520 Anfoka, G.H., 2000. Benzo-(1,2,3)-thiadiazole-7-carbothioic acid *S*-methyl ester induces systemic
521 resistance in tomato (*Lycopersicon esculentum*. Mill cv. Vollendung) to *Cucumber mosaic*
522 *virus*. Crop Prot. 19, 401–405. [https://doi.org/10.1016/S0261-2194\(00\)00031-4](https://doi.org/10.1016/S0261-2194(00)00031-4).

523 Carr, J.P., Lewsey, M.G., Palukaitis, P., 2010. Signaling in induced resistance, in: Carr, J.P.,
524 Loebenstein, G. (Eds.), Advances in Virus Research. Academic Press, Burlington, pp. 57–121.

525 Chirkov, S.N., Il'ina, A.V., Surgucheva, N.A., Letunova, E.V., Varitsev, Y.A., Tatarinova, N.Y.,
526 Varlamov, V.P., 2001. Effect of chitosan on systemic viral infection and some defense
527 responses in potato plants. Russ. J. Plant Physiol. 48, 774–779.
528 <https://doi.org/10.1023/A:1012508625017>.

529 Coqueiro, D.S.O., Maraschin, M., Di Piero, R.M., 2011. Chitosan reduces bacterial spot severity
530 and acts in phenylpropanoid metabolism in tomato plants. J. Phytopathol. 159, 488–494.
531 <https://doi.org/10.1111/j.1439-0434.2011.01791.x>.

532 Doares, S.H., Syrovets, T., Weiler, E.W., Ryan, C.A., 1995. Oligogalacturonides and chitosan
533 activate plant defensive genes through the octadecanoid pathway. Proc. Natl. Acad. Sci. USA.
534 92, 4095–4098.

535 Edwardson, J.R., Christie, R.G., 1991. CRC Handbook of Viruses Infecting Legumes, CRC Press,
536 Boca Raton.

537 Feliziani, E., Landi, L., Romanazzi, G., 2015. Preharvest treatments with chitosan and other
538 alternatives to conventional fungicides to control postharvest decay of strawberry. Carbohydr.
539 Polym. 132, 111–117. <https://doi.org/10.1016/j.carbpol.2015.05.078>.

540 Fraser, P.D., Bramley, P.M., 2004. The biosynthesis and nutritional uses of carotenoids. Prog. Lipid
541 Res. 43, 228–265. <https://doi.org/10.1016/j.plipres.2003.10.002>.

542 Gallitelli, D., 2000. The ecology of *Cucumber mosaic virus* and sustainable agriculture. *Virus Res.*
543 71, 9–21. [https://doi.org/10.1016/S0168-1702\(00\)00184-2](https://doi.org/10.1016/S0168-1702(00)00184-2).

544 Gallitelli, D., 1998. Present status of controlling *Cucumber mosaic virus*, in: Hadidi, A., Khetarpal,
545 R.K., Koganezawa, H. (Eds.), *Plant Virus Disease Control*. APS Press, St. Paul, pp. 507–523.

546 Giorio, G., Stigliani, A.L., D'Ambrosio, C., 2008. Phytoene synthase genes in tomato (*Solanum*
547 *lycopersicum* L.) - new data on the structures, the deduced amino acid sequences and the
548 expression patterns. *FEBS J.* 275, 527–535. <https://doi.org/10.1111/j.1742-4658.2007.06219.x>.

549 Hassan, O., Chang, T., 2017. Chitosan for eco-friendly control of plant disease. *Asian J. Plant*
550 *Pathol.* 11, 53–70. <https://doi.org/10.3923/ajppaj.2017.53.70>.

551 Ibdah, M., Dubey, N.K., Eizenberg, H., Dabour, Z., Abu-Nassar, J., Gal-On, A., Aly, R., 2014.
552 *Cucumber mosaic virus* as a carotenoid inhibitor reducing *Phelipanche aegyptiaca* infection in
553 tobacco plants. *Plant Signal. Behav.* 9, e972146. <http://dx.doi.org/10.4161/psb.32096>.

554 Ipper, N.S., Cho, S., Lee, S.H., Cho, J.M., Hur, J.H., Lim, C.K., 2008. Antiviral activity of the
555 exopolysaccharide produced by *Serratia* sp. strain Gsm01 against *Cucumber mosaic virus*. *J.*
556 *Microbiol. Biotechnol.* 18, 67–73.

557 Iriti, M., Picchi, V., Rossoni, M., Gomarasca, S., Ludwig, N., Gargano, M., Faoro, F., 2009.
558 Chitosan antitranspirant activity is due to abscisic acid-dependent stomatal closure. *Environ.*
559 *Exp. Bot.* 66, 493–500. <https://doi.org/10.1016/j.envexpbot.2009.01.004>.

560 Iriti, M., Varoni, E.M., 2015. Chitosan-induced antiviral activity and innate immunity in plants.
561 *Environ. Sci. Pollut. Res.* 22, 2935–2944. <https://doi.org/10.1007/s11356-014-3571-7>.

562 Jia, X., Meng, Q., Zeng, H., Wang, W., Yin, H., 2016. Chitosan oligosaccharide induces resistance
563 to *Tobacco mosaic virus* in *Arabidopsis* via the salicylic acid-mediated signalling pathway.
564 *Sci. Rep.* 6, 26144. <https://doi.org/10.1038/srep26144>.

565 Kumar, S., Chauhan, P.S., Agrawal, L., Raj, R., Srivastava, A., Gupta, S., Mishra, S.K., Yadav, S.,
566 Singh, P.C., Raj, S.K., Nautiyal, C.S., 2016. *Paenibacillus lentimorbus* inoculation enhances

567 tobacco growth and extenuates the virulence of *Cucumber mosaic virus*. PLoS One. 11,
568 e0149980. <https://doi.org/10.1371/journal.pone.0149980>.

569 Kumaraswamy, R.V., Kumari, S., Choudhary, R.C., Pal, A., Raliya, R., Biswas, P., Saharan, V.,
570 2018. Engineered chitosan based nanomaterials: bioactivities, mechanisms and perspectives in
571 plant protection and growth. Int. J. Biol. Macromol. 113, 494–506.
572 <https://doi.org/10.1016/j.ijbiomac.2018.02.130>.

573 Lee, S.W., Heinz, R., Robb, J., Nazar, R.N., 1994. Differential utilization of alternate initiation sites
574 in a plant defense gene responding to environmental stimuli. Eur. J. Biochem. 226, 109–114.
575 <https://doi.org/10.1111/j.1432-1033.1994.0t109.x>.

576 Liu, D., Jiao, S., Cheng, G., Li, X., Pei, Z., Pei, Y., Yin, H., Du, Y., 2018. Identification of chitosan
577 oligosaccharides binding proteins from the plasma membrane of wheat leaf cell. Int. J. Biol.
578 Macromol. 111, 1083–1090. <https://doi.org/10.1016/j.ijbiomac.2018.01.113>.

579 Liu, H., Du, Y., Wang, X., Sun, L., 2004. Chitosan kills bacteria through cell membrane damage.
580 Int. J. Food Microbiol. 95, 147–155. <https://doi.org/10.1016/j.ijfoodmicro.2004.01.022>.

581 Malerba, M., Cerana, R., 2016. Chitosan effects on plant systems. Int. J. Mol. Sci. 17, 996.
582 <https://doi.org/10.3390/ijms17070996>.

583 Marler, T.E., Mickelbart, M.V., Quitugua, R., 1993. Papaya ringspot virus influences net gas
584 exchange of papaya leaves. HortScience. 28, 322–324.

585 Mayda, E., Marqués, C., Conejero, V., Vera, P., 2000. Expression of a pathogen-induced gene can
586 be mimicked by auxin insensitivity. Mol. Plant Microbe Interact. 13, 23–31.
587 <https://doi.org/10.1094/MPMI.2000.13.1.23>.

588 Mejía-Teniente, L., de Dalia Duran-Flores, F., Chapa-Oliver, A.M., Torres-Pacheco, I., Cruz-
589 Hernández, A., González-Chavira, M.M., Ocampo-Velázquez, R.V., Guevara-González, R.G.,
590 2013. Oxidative and molecular responses in *Capsicum annuum* L. after hydrogen peroxide,
591 salicylic acid and chitosan foliar applications. Int. J. Mol. Sci. 14, 10178–10196.

592 <https://doi.org/10.3390/ijms140510178>.

593 Meléndez-Martínez, A.J., Fraser, P.D., Bramley, P.M., 2010. Accumulation of health promoting
 594 phytochemicals in wild relatives of tomato and their contribution to *in vitro* antioxidant
 595 activity. *Phytochemistry*. 71, 1104–1114. <https://doi.org/10.1016/j.phytochem.2010.03.021>.

596 Mou, Z., Fan, W., Dong, X., 2003. Inducers of plant systemic acquired resistance regulate NPR1
 597 function through redox changes. *Cell*. 113, 935–944. [https://doi.org/10.1016/S0092-](https://doi.org/10.1016/S0092-8674(03)00429-X)
 598 8674(03)00429-X.

599 Murchie, E.H., Lawson, T., 2013. Chlorophyll fluorescence analysis: a guide to good practice and
 600 understanding some new applications. *J. Exp. Bot.* 64, 3983–3998.
 601 <https://doi.org/10.1093/jxb/ert208>.

602 Nagorskaya, V., Reunov, A., Lapshina, L., Davydova, V., Yermak, I., 2014. Effect of chitosan on
 603 *Tobacco mosaic virus* (TMV) accumulation, hydrolase activity, and morphological
 604 abnormalities of the viral particles in leaves of *N. tabacum* L. cv. Samsun. *Virol. Sin.* 29, 250–
 605 256. <https://doi.org/10.1007/s12250-014-3452-8>.

606 Nie, P., Li, X., Wang, S., Guo, J., Zhao, H., Niu, D., 2017. Induced systemic resistance against
 607 *Botrytis cinerea* by *Bacillus cereus* AR156 through a JA/ET- and *NPR1*-dependent signaling
 608 pathway and activates PAMP-triggered immunity in *Arabidopsis*. *Front. Plant Sci.* 8, 238.
 609 <https://doi.org/10.3389/fpls.2017.00238>.

610 Niu, D., Wang, X., Wang, Y., Song, X., Wang, J., Guo, J., Zhao, H., 2016. *Bacillus cereus* AR156
 611 activates PAMP-triggered immunity and induces a systemic acquired resistance through a
 612 *NPR1*-and SA-dependent signaling pathway. *Biochem. Biophys. Res. Commun.* 469, 120–125.
 613 <https://doi.org/10.1016/j.bbrc.2015.11.081>.

614 Ogawa, D., Nakajima, N., Seo, S., Mitsuhashi, I., Kamada, H., Ohashi, Y., 2006. The phenylalanine
 615 pathway is the main route of salicylic acid biosynthesis in *Tobacco mosaic virus*-infected
 616 tobacco leaves. *Plant Biotechnol.* 23, 395–398.

617 <https://doi.org/10.5511/plantbiotechnology.23.395>.

618 Pandey, V.P., Awasthi, M., Singh, S., Tiwari, S., Dwivedi, U.N., 2017. A comprehensive review on
619 function and application of plant peroxidases. *Biochem. Anal. Biochem.* 6, 308.
620 <https://doi.org/10.4172/2161-1009.1000308>.

621 Petutschnig, E.K., Jones, A.M.E., Serazetdinova, L., Lipka, U., Lipka, V., 2010. The lysin motif
622 receptor-like kinase (LysM-RLK) CERK1 is a major chitin-binding protein in *Arabidopsis*
623 *thaliana* and subject to chitin-induced phosphorylation. *J. Biol. Chem.* 285, 28902–28911.
624 <https://doi.org/10.1074/jbc.M110.116657>.

625 Povero, G., Loreti, E., Pucciariello, C., Santaniello, A., Di Tommaso, D., Di Tommaso, G., Kapetis,
626 D., Zolezzi, F., Piaggese, A., Perata, P., 2011. Transcript profiling of chitosan-treated
627 *Arabidopsis* seedlings. *J. Plant Res.* 124, 619–629. <https://doi.org/10.1007/s10265-010-0399-1>.

628 Salachna, P., Byczyńska, A., Jeziorska, I., Udycz, E., 2017. Plant growth of *Verbena bonariensis* L.
629 after chitosan, gellan gum or iota-carrageenan foliar applications. *World Sci. News* 62,
630 111–123.

631 Sharif, R., Mujtaba, M., Ur Rahman, M., Shalmani, A., Ahmad, H., Anwar, T., Tianchan, D.,
632 Wang, X., 2018. The multifunctional role of chitosan in horticultural crops; a review.
633 *Molecules* 23, 872. <https://doi.org/10.3390/molecules23040872>.

634 Shi, J., Yu, L., Song, B., 2018. Proteomics analysis of Xiangcaoliusuobingmi-treated *Capsicum*
635 *annuum* L. infected with *Cucumber mosaic virus*. *Pest. Biochem. Physiol.* 149, 113–122.
636 <https://doi.org/10.1016/j.pestbp.2018.06.008>.

637 Sivakumar, D., Bill, M., Korsten, L., Thompson, K., 2016. Integrated application of chitosan
638 coating with different postharvest treatments in the control of postharvest decay and
639 maintenance of overall fruit quality, in: Bautista-Baños, S., Romanazzi, G., Jiménez-Aparicio,
640 A. (Eds.), *Chitosan in the Preservation of Agricultural Commodities*. Academic Press,
641 Cambridge, pp. 127–153.

642 Sofo, A., Bochicchio, R., Amato, M., Rendina, N., Vitti, A., Nuzzaci, M., Altamura, M.M., Falasca,
643 G., Della Rovere, F., Scopa, A., 2017. Plant architecture, auxin homeostasis and phenol
644 content in *Arabidopsis thaliana* grown in cadmium- and zinc-enriched media. J. Plant Physiol.
645 216, 174–180. <https://doi.org/10.1016/j.jplph.2017.06.008>.

646 Spoel, S.H., Koornneef, A., Claessens, S.M.C., Korzelius, J.P., Van Pelt, J.A., Mueller, M.J.,
647 Buchala, A.J., Métraux, J.P., Brown, R., Kazan, K., Van Loon, L.C., Dong, X., Pieterse,
648 C.M.J., 2003. NPR1 modulates cross-talk between salicylate- and jasmonate-dependent
649 defense pathways through a novel function in the cytosol. Plant Cell. 15, 760–770.
650 <https://doi.org/10.1105/tpc.009159>.

651 Van, S.N., Minh, H.D., Anh, D.N., 2013. Study on chitosan nanoparticles on biophysical
652 characteristics and growth of Robusta coffee in green house. Biocatal. Agric. Biotechnol. 2,
653 289–294. <https://doi.org/10.1016/j.bcab.2013.06.001>.

654 Vitti, A., La Monaca, E., Sofo, A., Scopa, A., Cuypers, A., Nuzzaci, M., 2015. Beneficial effects of
655 *Trichoderma harzianum* T-22 in tomato seedlings infected by *Cucumber mosaic virus* (CMV).
656 BioControl. 60, 135–147. <https://doi.org/10.1007/s10526-014-9626-3>.

657 Vitti, A., Pellegrini, E., Nali, C., Lovelli, S., Sofo, A., Valerio, M., Scopa, A., Nuzzaci, M., 2016.
658 *Trichoderma harzianum* T-22 induces systemic resistance in tomato infected by *Cucumber*
659 *mosaic virus*. Front. Plant Sci. 7, 1520. <https://doi.org/10.3389/fpls.2016.01520>.

660 Wu, Y., Zhang, D., Chu, J.Y., Boyle, P., Wang, Y., Brindle, I.D., De Luca, V., Després, C., 2012.
661 The *Arabidopsis* NPR1 protein is a receptor for the plant defense hormone salicylic acid. Cell
662 Rep. 1, 639–647. <https://doi.org/10.1016/j.celrep.2012.05.008>.

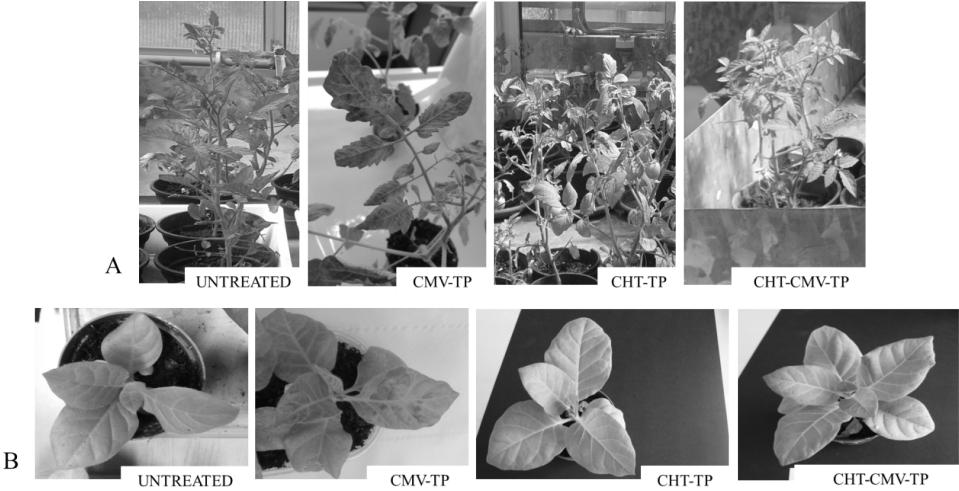
663 Xing, K., Zhu, X., Peng, X., Qin, S., 2015. Chitosan antimicrobial and eliciting properties for pest
664 control in agriculture: a review. Agron. Sustain. Dev. 35, 569–588.
665 <https://doi.org/10.1007/s13593-014-0252-3>.

666 Zhang, D., Wang, H., Hu, Y., Liu, Y., 2015. Chitosan controls postharvest decay on cherry tomato

fruit possibly via the mitogen-activated protein kinase signaling pathway. *J. Agric. Food Chem.* 63, 7399–7404. <https://doi.org/10.1021/acs.jafc.5b01566>.

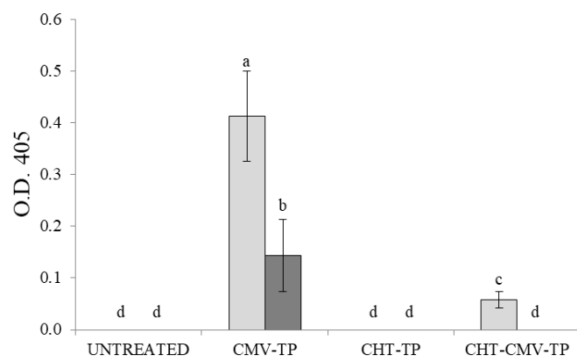
Zhao, J., Zhang, X., Hong, Y., Liu, Y., 2016. Chloroplast in plant-virus interaction. *Front. Microbiol.* 7, 1565. <https://doi.org/10.3389/fmicb.2016.01565>.

692 Figure 1. Phenotypical observations of symptoms induced by *Cucumber mosaic virus* (CMV) 20 days and 11 days after
693 CMV inoculation of representative A) *Solanum lycopersicum* var. *cerasiforme* and B) *Nicotiana tabacum* cv Xanthi
694 plants, respectively. Four different experimental conditions: untreated plants; plants inoculated with CMV (CMV-TP);
695 plants treated with CHT (CHT-TP); plants treated with CHT and then inoculated with CMV 24 h after CHT treatment
696 (CHT-CMV-TP).
697



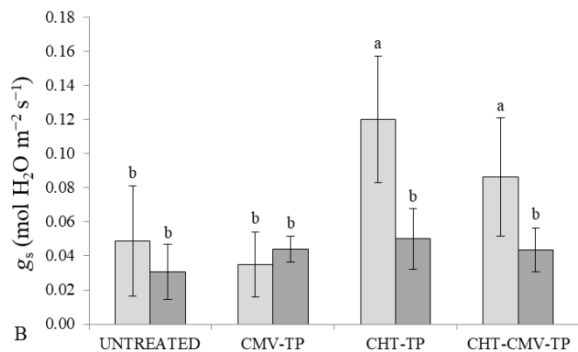
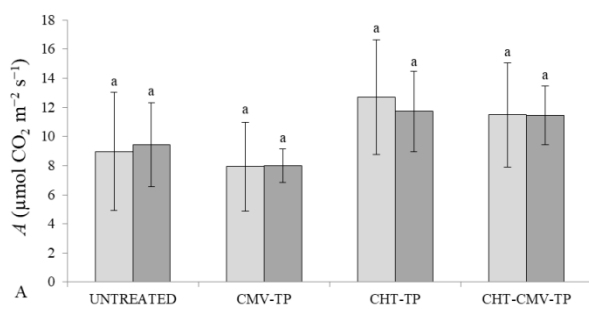
698
699

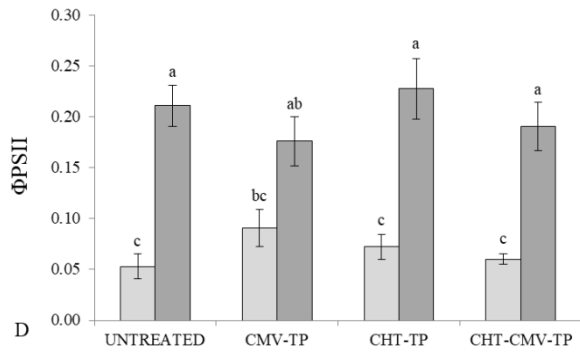
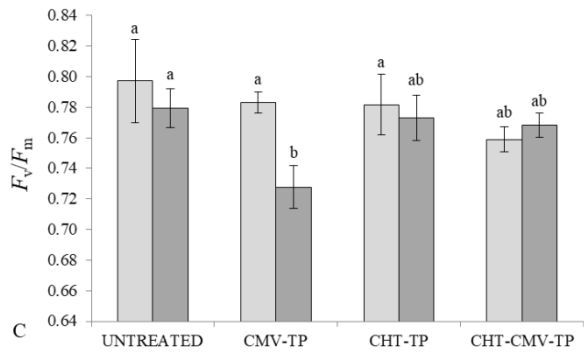
700 Figure 2. *Cucumber mosaic virus* (CMV) load 20 days (light grey bars) and 90 days (dark grey bars) after CMV
 701 inoculation of tomato plants. Mean values ($n = 6$) are represented. Standard deviations are represented by bars.
 702 Significant differences ($P \leq 0.05$) among treatments and time are indicated by different letters, according to non-
 703 parametric two-way ANOVA. Four different experimental conditions: untreated plants; plants inoculated with CMV
 704 (CMV-TP); plants treated with CHT (CHT-TP); plants treated with CHT and then inoculated with CMV 24 h after CHT
 705 treatment (CHT-CMV-TP).
 706



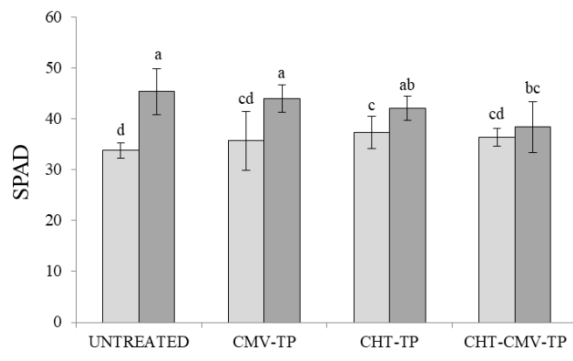
707
 708

709 Figure 3. Gas exchange and chlorophyll fluorescence determinations. A) Photosynthetic activity (A), B) stomatal
 710 conductance to water vapor (g_s), C) maximal quantum yield of PSII (F_v/F_m) and D) quantum yield of PSII (ϕ PSII),
 711 measured in 2- (light grey bars) and 4-month-old (dark grey bars) tomato plants. Mean values ($n \geq 6$ for gas exchange; n
 712 $= 4$ for chlorophyll fluorescence) are represented. Standard deviations are represented by bars. Significant differences
 713 ($P \leq 0.05$) among treatments and time are indicated by different letters, according to parametric and non-parametric (g_s)
 714 two-way ANOVA. Four different experimental conditions: untreated plants; plants inoculated with CMV (CMV-TP);
 715 plants treated with CHT (CHT-TP); plants treated with CHT and then inoculated with CMV 24 h after CHT treatment
 716 (CHT-CMV-TP).



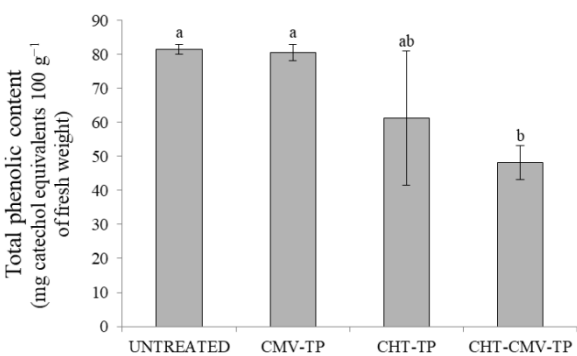


722 Figure 4. Chlorophyll content (SPAD) measured in 2- (light grey bars) and 4-month-old (dark grey bars) tomato plants.
 723 Mean values ($n = 6$) are represented. Standard deviations are represented by bars. Significant differences ($P \leq 0.05$)
 724 among treatments and time are indicated by different letters, according to non-parametric two-way ANOVA. Four
 725 different experimental conditions: untreated plants; plants inoculated with CMV (CMV-TP); plants treated with CHT
 726 (CHT-TP); plants treated with CHT and then inoculated with CMV 24 h after CHT treatment (CHT-CMV-TP).



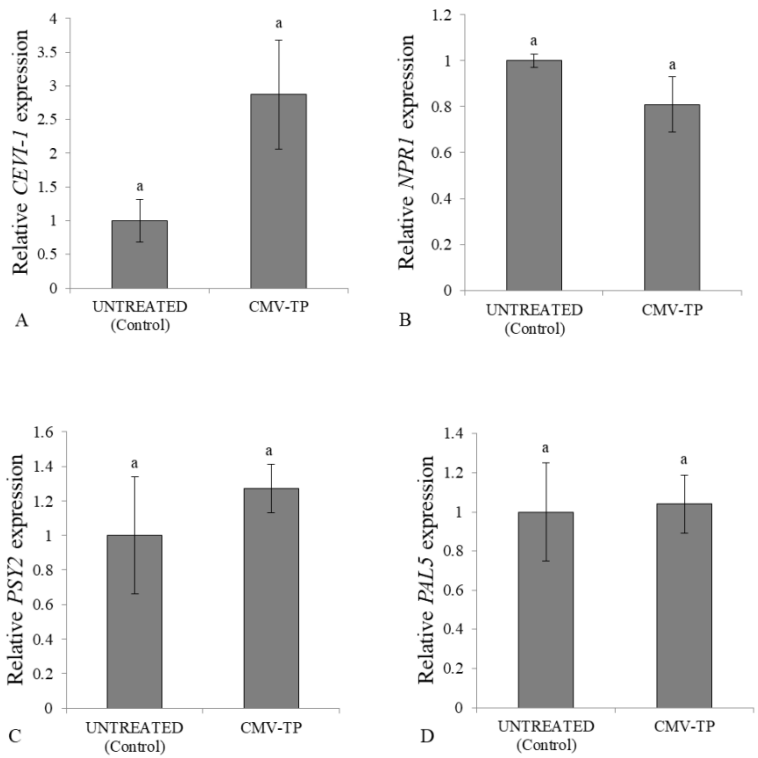
727
 728

729 Figure 5. Total phenolic content of tomato leaves. Mean values ($n = 4$) are represented. Standard deviations are
 730 represented by bars. Significant differences ($P \leq 0.05$) among treatments are indicated by different letters, according to
 731 non-parametric one-way ANOVA. Four different experimental conditions: untreated plants; plants inoculated with
 732 CMV (CMV-TP); plants treated with CHT (CHT-TP); plants treated with CHT and then inoculated with CMV 24 h
 733 after CHT treatment (CHT-CMV-TP).



734
 735

736 Figure 6. Genes expression in CMV-TP relatively expressed to the Untreated tomato plants. A) peroxidase (*CEVI-1*), B)
 737 non-expressor of pathogenesis-related genes 1 (*NPR1*), C) phytoene synthase 2 (*PSY2*) and D) phenylalanine
 738 ammonia lyase (*PAL5*). Mean values ($n = 4$) are represented. Standard errors are represented by bars. Significant
 739 differences ($P \leq 0.05$) among treatments are indicated by different letters, according to parametric one-way ANOVA.
 740 Two different experimental conditions: untreated plants; plants inoculated with CMV (CMV-TP).



744 Figure 7. Genes expression in CHT-TP and CHT-CMV-TP relatively expressed to the CMV-TP (tomato plants). A)
 745 peroxidase (*CEVI-1*), B) non-expressor of pathogenesis-related genes 1 (*NPR1*), C) phytoene synthase 2 (*PSY2*) and D)
 746 phenylalanine ammonia lyase (*PAL5*). Mean values ($n = 4$) are represented. Standard errors are represented by bars.
 747 Significant differences ($P \leq 0.05$) among treatments are indicated by different letters, according to parametric one-
 748 way ANOVA. Three different experimental conditions: plants inoculated with CMV (CMV-TP); plants treated with
 749 CHT (CHT-TP); plants treated with CHT and then inoculated with CMV 24 h after CHT treatment (CHT-CMV-TP).

